

# Squeezed state protection of fine structure in “Poor Man’s Majorana” via quantum spin coupling

J.E. Sanches,<sup>1,\*</sup> L.T. Lustosa,<sup>1</sup> L.S. Ricco,<sup>2</sup> H. Sigurðsson,<sup>2,3</sup>  
M. de Souza,<sup>4</sup> M.S. Figueira,<sup>5</sup> E. Marinho Jr.,<sup>1,†</sup> and A.C. Seridonio<sup>1,‡</sup>

<sup>1</sup>São Paulo State University (Unesp), School of Engineering,  
Department of Physics and Chemistry, 15385-007, Ilha Solteira-SP, Brazil

<sup>2</sup>Science Institute, University of Iceland, Dunhagi-3, IS-107, Reykjavik, Iceland

<sup>3</sup>Institute of Experimental Physics, Faculty of Physics,  
University of Warsaw, ulica Pasteura 5, PL-02-093 Warsaw, Poland

<sup>4</sup>São Paulo State University (Unesp), IGCE, Department of Physics, 13506-970, Rio Claro-SP, Brazil

<sup>5</sup>Instituto de Física, Universidade Federal Fluminense, 24210-340, Niterói, Rio de Janeiro, Brazil

The “Poor Man’s Majorana” [Phys. Rev. B 86, 134528 (2012)] devoid of topological protection has been theoretically predicted to rely on the minimal Kitaev chain. Afterward, a pair of superconducting and *spinless* quantum dots turned the proposal practicable and differential conductance pinpointed consistent fingerprints with such a scenario [Nature 614, 445 (2023) and Nature 630, 329 (2024)]. In this work, we propose a model wherein the “Poor Man’s Majorana” presents protection when one of the dots is exchange coupled to a quantum spin. If this quantum dot is perturbed by tuning the exchange coupling, the well-known spill over-like behavior of this *Majorana* surprisingly remains unchanged, and solely half of the fine structure is unexpectedly viewed. As a matter of fact, the “Poor Man’s Majorana” zero mode consists in squeezing of the other half at zero frequency, which imposes its pinning there and prevents the mixing of the mode with the explicit fine structure. We claim that if the supposed unavoidable split of the zero mode by the fine structure is unexpectedly absent, then the “Poor Man’s Majorana” can be considered robust against the quantum spin. In this way, it becomes protected and the lack of topological protection paradigm of the “Poor Man’s Majorana” has been revisited, pushing this seemingly well-established issue into a new direction.

*Introduction.*— Proposed by Ettore Majorana in 1937, Majorana fermions (MFs) consist in real solutions of the Dirac equation in which the particle is equivalent to its antiparticle[1]. Particularly, in Condensed Matter Physics, such solutions emerge as quasiparticle excitations known as Majorana bound states (MBSs), which are zero-energy modes attached to the edges of topological superconductors[2–27]. Within such a context, Alexei Kitaev in 2001, with the so-called Kitaev toy model[28], idealized a linear system characterized by this exotic superconductivity, which is of *p-wave*-type symmetry, being responsible for the appearance of these non-local MBSs. Such MBSs, indeed, once showing topological protection, could be employed as building-blocks for the fault-tolerant quantum computing[2, 23, 29]. Consequently, the last decade has witnessed a plethora of theoretical and experimental efforts in exploring potential hosts of MBSs for technological purposes[2, 4, 21, 23, 28–33].

In this route, it is well-known that, in principle, the realization of the Kitaev toy model and later on, MBSs at the system boundaries, depend on the mixing of special ingredients, such as the superconducting proximity-effect, due to an *s-wave* platform, Zeeman field and spin-orbit interaction, in particular, over certain systems, such as linear lattices of magnetic atoms[9, 14, 33–42] and

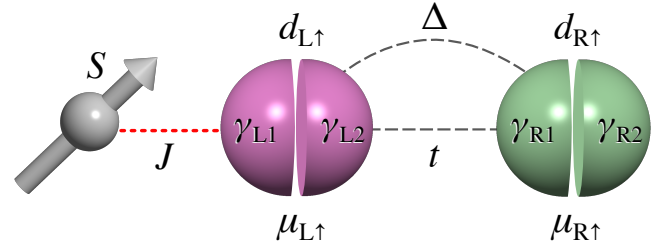


Figure 1. Sketch of the minimal Kitaev chain modified by a quantum spin  $S$  exchange coupled via  $J$  to the left QD (purple sphere) with chemical potential  $\mu_{L\uparrow}$  in the electronic basis  $d_{L\uparrow}$ , which is built-up by the couple of MBSs  $\gamma_{L1}$  and  $\gamma_{L2}$ . For the right QD (green sphere), we have similarly  $\mu_{R\uparrow}$ ,  $d_{R\uparrow}$ ,  $\gamma_{R1}$  and  $\gamma_{R2}$ . Both the QDs are connected to each other by ECT and CAR given by  $t$  and  $\Delta$  terms, respectively. For  $\Delta = t$ ,  $\mu_{L\uparrow} = \mu_{R\uparrow} = 0$  and  $J \neq 0$ , the zero-energy mode of the “Poor Man’s Majorana”  $\gamma_{L1}$  is due to the squeezing of half of the fine structure induced by the quantum spin. As the other half does not couple to this mode, it becomes protected.

semiconducting nanowires[21, 25–27, 29, 30, 43]. However, despite these well-established theoretical recipes in bringing forth MBSs, their detection remains elusive once other phenomena can misrepresent the MBS signature, such as disorder and Andreev reflection[2, 23]. Both of these phenomena could also yield a zero-energy mode, but topologically trivial instead.

Alternatively, the recent experiments reported by Refs.[44–46] with quantum dots (QDs) have pointed out compatible fingerprints with the so-called “Poor Man’s

\* corresponding author:jose.sanches@unesp.br

† corresponding author:enesio.marinho@unesp.br

‡ corresponding author:antonio.seridonio@unesp.br

*Majorana*” (“*Poor M.M.*”)[47–52]. Such a designation was introduced by M. Leijnse and K. Flensberg to label a MBS without topological protection[47]. They conjectured that in the minimal Kitaev chain, namely that one with two sites, the MBS with the nickname “*Poor M.M.*” could be feasible. Such quasiparticle could emerge due to the mixing of two spin-polarized grounded QDs equally coupled by electronic co-tunneling (ECT) and crossed Andreev reflection (CAR) processes. In this *sweet spot*[47], the isolation of the MBSs would occur in spatially distinct QDs of this dimer. Unfortunately, due to the lack of topological protection of these MBSs if one of the QDs is found not grounded, the MBS initially isolated at one QD then spills over the other.[47].

In this work, we reveal that the “*Poor M.M.*” exhibits a distinct protection if one QD is exchange coupled to a quantum spin. By perturbing this QD via variations of the exchange coupling, the well-established spill over-like behavior of the “*Poor M.M.*” counterintuitively remains, in particular with the mode pinned at zero frequency and fully decoupled from the fine structure due to the quantum spin, which is half of the entire spectrum. Surprisingly, the other half of the fine structure is found squeezed as the zero-energy mode of the “*Poor M.M.*”, thus imposing the pinning of such a mode at zero frequency and then, protecting it against the other half.

Our result makes explicit if the “*Poor M.M.*” is still observed arising from this spill over-like behavior, the protection against a quantum spin is a concrete feature. This is due to the half of the fine structure clearly detached from this MBS, while the other half squeezed at zero frequency leads to the formation of the “*Poor M.M.*” itself. These findings challenge the lack of topological protection paradigm of the “*Poor M.M.*” and provide a new direction for research on this matter.

*The Model.*- We consider the system schematically shown by Fig.1 and inspired in the experiments reported by Refs.[44, 45]. Distinctly, we account for the fine structure due to a quantum spin  $S$ . The simplest way to introduce such is via the *Ising-like* Hamiltonian  $JS^z s^z$ [53]. To that end, we adopt the exchange term  $J$ ,  $S^z = \sum_m m|m\rangle\langle m|$  wherein  $m = [-S, -S + 1, \dots, S - 1, S]$  and for the left QD the *spin-z* operator  $s^z = \frac{1}{2} \sum_{\sigma} \sigma d_{L\sigma}^{\dagger} d_{L\sigma}$ , with  $d_{L\sigma}^{\dagger}$  ( $d_{L\sigma}$ ) as the creation (annihilation) operator and  $\sigma = \pm 1$  ( $\uparrow, \downarrow$ ). For the right QD, we have  $d_{R\sigma}^{\dagger}$  ( $d_{R\sigma}$ ).

The QDs are found within the *spinless* regime, where we arbitrary choose the spin-up channel  $\sigma = \uparrow$  as relevant, due to an imposed large Zeeman splitting. Most relevant, such a dimer of QDs then constitutes the minimal Kitaev chain, being the QDs linked to each other by means of ECT and CAR mechanisms, ruled by the hopping  $t$  and superconducting pairing  $\Delta$  terms, respectively. This scenario is mimicked by the effective Hamiltonian

$$\mathcal{H} = (\mu_{L\uparrow} + \frac{J}{2}S^z)d_{L\uparrow}^{\dagger}d_{L\uparrow} + \mu_{R\uparrow}d_{R\uparrow}^{\dagger}d_{R\uparrow} + (td_{L\uparrow}d_{R\uparrow}^{\dagger} + \Delta d_{L\uparrow}d_{R\uparrow} + \text{H.c.}), \quad (1)$$

where  $\mu_{L\uparrow}$  ( $\mu_{R\uparrow}$ ) represents the chemical potential for the

QD  $\alpha = L, R$ . Both the electronic operators of the chain can be projected onto the MBS basis  $\gamma_{L1(L2)}$  and  $\gamma_{R1(R2)}$  for the left and the right QDs, respectively. To perform such, it is imperative to evoke the relations  $d_{L\uparrow} = (\gamma_{L1} + i\gamma_{L2})/\sqrt{2}$  and  $d_{R\uparrow} = (\gamma_{R1} + i\gamma_{R2})/\sqrt{2}$ . By considering the “*Majorana chain regime*”  $t = \Delta$  in Eq.(1) the Hamiltonian turns into

$$\mathcal{H} = i(\mu_{L\uparrow} + JS^z)\gamma_{L1}\gamma_{L2} + i\mu_{R\uparrow}\gamma_{R1}\gamma_{R2} + i2t\gamma_{L2}\gamma_{R1}, \quad (2)$$

from where it is notorious the *sweet spot*[47]  $\mu_{\alpha\uparrow} = \mu_{\bar{\alpha}\uparrow} = J = 0$ , being  $\bar{\alpha} = L(R)$  for the opposite QD  $\alpha = R(L)$ , characterized by the spatially apart isolated MBSs  $\gamma_{L1}$  and  $\gamma_{R2}$  at the left and right QDs, respectively, once such quasiparticles do not enter into the Hamiltonian. As we know, these MBSs are the so-called “*Poor M. Ms.*”[44, 45, 47]. To understand such, for instance, suppose that  $\mu_{R\uparrow}$  is placed off the *sweet spot*. This allows the spectral amplitude of the zero-energy mode of  $\gamma_{R2}$  from the right QD to spill over the left one, in particular on  $\gamma_{L2}$ , in such a way that can be visualized together with  $\gamma_{L1}$ . As part of  $\gamma_{R2}$  is found at the left QD, the nickname for the MBS  $\gamma_{R2}$  is “*Poor M.M.*”, once the topological protection is lacking.

We reveal by considering  $\mu_{\alpha\uparrow} = \mu_{\bar{\alpha}\uparrow} = 0$  and  $J \neq 0$  in the “*Majorana chain regime*” that the zero-energy mode of the “*Poor M.M.*” consists the feature under protection against the  $J$  coupling. It is well-known that, due to a quantum spin  $S$ , the lifting of the energy spectrum per level into a  $2S + 1$  fine structure is expected. The zero-energy mode of the “*Poor M.M.*” then persists even when deviating from the *sweet spot*, in particular by  $J$  and the fine structure is reduced by half. Equivalently, we perform the break down of the *sweet spot*, but the zero-energy mode of the “*Poor M.M.*” counterintuitively remains pinned and does not belong to the renormalized fine structure. Indeed, the other half of the fine structure squeezes as the zero-energy mode of the “*Poor M.M.*” and ensures its pinning at  $\omega = 0$ , thus forbidding the mixing with the explicit part of the spectrum.

In order to uncover the physical mechanisms within the “*Poor M.M. regime*” the evaluation of frequency dependent retarded Green’s functions (GFs) for the QDs  $\alpha$  are timely, once they dictate the differential conductance[44, 45]. To this end, we should consider the ordinary spectral densities  $\mathcal{A}_{d_{\alpha\uparrow}d_{\alpha\uparrow}^{\dagger}}(\omega) = (-1/\pi)\text{Im}\langle\langle d_{\alpha\uparrow}; d_{\alpha\uparrow}^{\dagger} \rangle\rangle$  and  $\mathcal{A}_{d_{\alpha\uparrow}^{\dagger}d_{\alpha\uparrow}}(\omega) = (-1/\pi)\text{Im}\langle\langle d_{\alpha\uparrow}^{\dagger}; d_{\alpha\uparrow} \rangle\rangle$ , where  $\langle\langle A; B \rangle\rangle$  stands for the corresponding GF. The anomalous GFs  $\mathcal{A}_{d_{\alpha\uparrow}^{\dagger}d_{\alpha\uparrow}^{\dagger}}(\omega) = (-1/\pi)\text{Im}\langle\langle d_{\alpha\uparrow}^{\dagger}; d_{\alpha\uparrow}^{\dagger} \rangle\rangle$  and  $\mathcal{A}_{d_{\alpha\uparrow}d_{\alpha\uparrow}}(\omega) = (-1/\pi)\text{Im}\langle\langle d_{\alpha\uparrow}; d_{\alpha\uparrow} \rangle\rangle$  should be taken into account too. As shown below, they determine the MBS component  $\mathcal{A}_{\gamma_{\alpha j}}(\omega) = (-1/\pi)\text{Im}\langle\langle \gamma_{\alpha j}; \gamma_{\alpha j} \rangle\rangle$  of the QD. With it, we are able to quantify clearly the MBS from the QD  $\alpha$  that spills over the opposite QD  $\bar{\alpha}$  when the system is driven off the *sweet spot*[44, 45, 47]. From  $\gamma_{L1(L2)}$  and  $\gamma_{R1(R2)}$ ,

we obtain the GF as follows

$$\begin{aligned} \langle\langle \gamma_{\alpha j}; \gamma_{\alpha j} \rangle\rangle &= \frac{1}{2} [\langle\langle d_{\alpha\uparrow}^\dagger; d_{\alpha\uparrow}^\dagger \rangle\rangle + \langle\langle d_{\alpha\uparrow}^\dagger; d_{\alpha\uparrow} \rangle\rangle] \\ &+ \epsilon_j (\langle\langle d_{\alpha\uparrow}^\dagger; d_{\alpha\uparrow}^\dagger \rangle\rangle + \langle\langle d_{\alpha\uparrow}; d_{\alpha\uparrow} \rangle\rangle), \end{aligned} \quad (3)$$

where  $\epsilon_j = +1, -1$  for  $j = 1, 2$ . Thus, the task of calculating the GFs of Eq.(3) can be achieved via the standard equation-of-motion (EOM) approach[54], which is summarized as

$$(\omega + i\Gamma)\langle\langle A; B \rangle\rangle = \langle\langle A; B \rangle\rangle_+ + \langle\langle [A, \mathcal{H}]; B \rangle\rangle, \quad (4)$$

where  $\Gamma$  mimics the natural broadening, supposed to be symmetric for simplicity, arising from the outside environment. By applying the EOM technique to Eq.(1) for  $t \neq \Delta$  we then find

$$\langle\langle d_{\alpha\uparrow}; d_{\alpha\uparrow}^\dagger \rangle\rangle = \frac{1}{2S+1} \sum_m \frac{1}{\omega + i\Gamma - \mu_{\alpha\uparrow} - \frac{Jm}{2}\delta_{\alpha L} - \Sigma_\alpha^+}, \quad (5)$$

$$\langle\langle d_{\alpha\uparrow}^\dagger; d_{\alpha\uparrow} \rangle\rangle = \frac{1}{2S+1} \sum_m \frac{1}{\omega + i\Gamma + \mu_{\alpha\uparrow} + \frac{Jm}{2}\delta_{\alpha L} - \Sigma_\alpha^-}, \quad (6)$$

$$\langle\langle d_{\alpha\uparrow}^\dagger; d_{\alpha\uparrow}^\dagger \rangle\rangle = \eta_\alpha \frac{1}{2S+1} \sum_m \frac{2t\Delta K_\alpha^-}{\omega + i\Gamma + \mu_{\alpha\uparrow} + \frac{Jm}{2}\delta_{\alpha L} - \Sigma_\alpha^-}, \quad (7)$$

and

$$\langle\langle d_{\alpha\uparrow}; d_{\alpha\uparrow} \rangle\rangle = \eta_\alpha \frac{1}{2S+1} \sum_m \frac{2t\Delta K_\alpha^+}{\omega + i\Gamma - \mu_{\alpha\uparrow} - \frac{Jm}{2}\delta_{\alpha L} - \Sigma_\alpha^+}, \quad (8)$$

where we used  $\langle\langle A; B \rangle\rangle = \sum_m \langle\langle A | m \rangle \langle m |; B \rangle\rangle$ , the thermal average  $\langle |m\rangle \langle m| \rangle = \frac{1}{2S+1}$ ,  $\delta_{\alpha L}$  as the Kronecker Delta and  $\eta_\alpha = -1, +1$  for  $\alpha = L, R$ , respectively. The self-energy correction due to the several couplings is  $\Sigma_\alpha^\pm = \tilde{K}_\alpha^\pm + (2t\Delta)^2 K_\alpha^\mp K_\alpha^\pm$ , with

$$\tilde{K}_\alpha^\pm = \frac{(\omega + i\Gamma)(t^2 + \Delta^2) \pm (\mu_{\alpha\uparrow} + \frac{Jm}{2}\delta_{\alpha L})(t^2 - \Delta^2)}{(\omega + i\Gamma)^2 - (\mu_{\alpha\uparrow} + \frac{Jm}{2}\delta_{\alpha L})^2}, \quad (9)$$

$$K_\alpha = \frac{\omega + i\Gamma}{(\omega + i\Gamma)^2 - (\mu_{\alpha\uparrow} + \frac{Jm}{2}\delta_{\alpha L})^2} \quad (10)$$

and

$$K_\alpha^\pm = \frac{K_\alpha}{\omega + i\Gamma \pm \mu_{\alpha\uparrow} \pm \frac{Jm}{2}\delta_{\alpha L} - \tilde{K}_\alpha^\mp}. \quad (11)$$

*Results.*- Throughout the analysis we set  $\mu_{L\uparrow} = 0$  and the “Majorana chain regime”  $t = \Delta = 1.5$  in arbitrary units for Figs.2, 3 and 4.

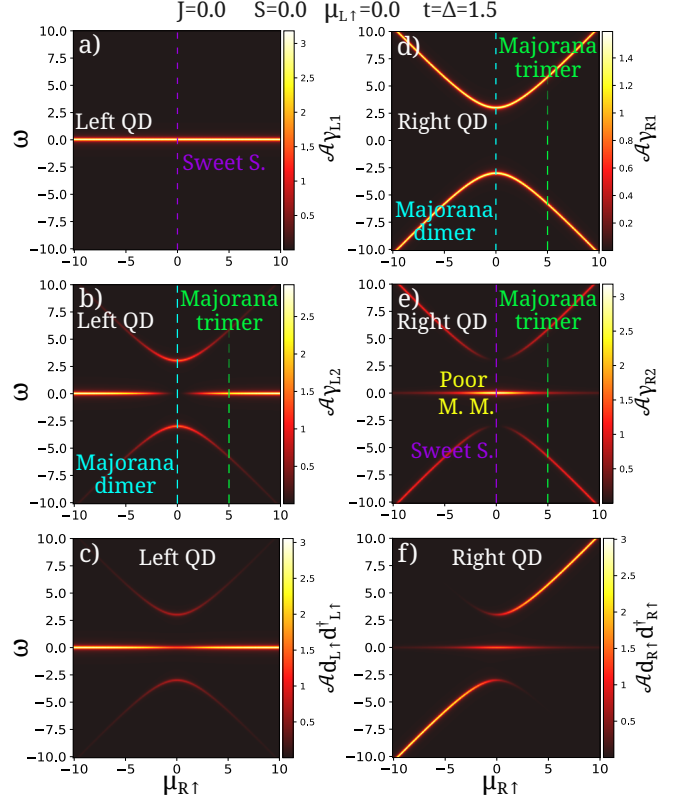


Figure 2. Color maps of  $\mathcal{A}_{d_{\alpha\uparrow}^\dagger d_{\alpha\uparrow}^\dagger}$  and  $\mathcal{A}_{\gamma_{\alpha j}}$  in the “Majorana chain regime” spanned by  $\omega$  and  $\mu_{R\uparrow}$ . Panel (a) exhibits a resonant zero-energy mode at  $\omega = 0$  in  $\mathcal{A}_{\gamma_{L1}}$  upon changing  $\mu_{R\uparrow}$ . In panel (b) for  $\mathcal{A}_{\gamma_{L2}}$  this mode is absent when  $\mu_{R\uparrow} = 0$ . Upper and lower arcs emerge. Panel (c) presents  $\mathcal{A}_{d_{L\uparrow}^\dagger d_{L\uparrow}^\dagger}$  made by the MBSs  $\gamma_{L1}$  and  $\gamma_{L2}$ . In panel (d) for  $\mathcal{A}_{\gamma_{R1}}$  we have only the upper and lower arcs. In case of panel (e) for  $\mathcal{A}_{\gamma_{R2}}$  there is the mode at  $\omega = 0$  and arcs appear off it. As the amplitude of  $\mathcal{A}_{\gamma_{R2}}$  at  $\omega = 0$  decreases while the corresponding of  $\mathcal{A}_{\gamma_{L2}}$  increases away from  $\mu_{R\uparrow} = 0$ , we conclude that  $\gamma_{R2}$  spills over  $\gamma_{L2}$ . The left QD is trivial with two locally zero-energy modes with  $\gamma_{L1}$  and  $\gamma_{L2}$  contributing simultaneously. The MBS  $\gamma_{R2}$  is then the “Poor Man’s Majorana” or simply “Poor M.M.”. On the other hand, the *sweet spot* (Sweet S.) occurs for fixed  $\mu_{R\uparrow} = 0$ , where we clearly see resonant zero-energy modes spatially apart at the left and right QDs, respectively. This appears via finite values at  $\omega = 0$  solely in  $\mathcal{A}_{\gamma_{L1}}$  and  $\mathcal{A}_{\gamma_{R2}}$ , in opposite to the corresponding null in  $\mathcal{A}_{\gamma_{L2}}$  and  $\mathcal{A}_{\gamma_{R1}}$ , respectively. Panel (f) shows  $\mathcal{A}_{d_{R\uparrow}^\dagger d_{R\uparrow}^\dagger}$  made by  $\gamma_{R1}$  and  $\gamma_{R2}$ . We call attention that such a scenario breaks down upon varying  $\mu_{R\uparrow}$  and thus leads to the “Poor M.M.”.

Fig.2 shows the spectral densities spanned by the frequency  $\omega$  and  $\mu_{R\uparrow}$ , with  $\mu_{L\uparrow} = J = 0$ . Panel (a) of Fig.2 exhibits  $\mathcal{A}_{\gamma_{L1}}$  for the left QD, where we see a resonant profile pinned at  $\omega = 0$  as a zero-energy mode upon tuning  $\mu_{R\uparrow}$ . It represents the isolated MBS  $\gamma_{L1}$  of the left QD (purple line cut), which is found decoupled from any MBS of the system due to the characteristic  $\mu_{L\uparrow} = 0$  in Eq.(2). At the *sweet spot* with

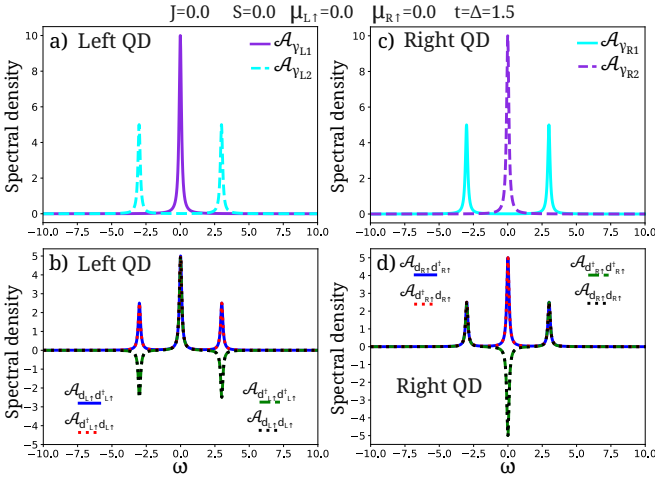


Figure 3. Spectral densities in the “Majorana chain regime” within the *sweet spot*. Panels (a) and (c) exhibit resonant zero-energy modes spatially apart at the left and right QDs, respectively. Such a feature can be seen in  $\mathcal{A}_{\gamma_{L1}}$  and  $\mathcal{A}_{\gamma_{R2}}$  at  $\omega = 0$ , while  $\mathcal{A}_{\gamma_{L2}}$  and  $\mathcal{A}_{\gamma_{R1}}$  show a split-peak structure due to the coupling  $i2t\gamma_{L2}\gamma_{R1}$  in Eq.(2). In panels (b) and (d) the ordinary spectral densities  $\mathcal{A}_{d_{\alpha\uparrow}d_{\alpha\uparrow}^\dagger}$  and  $\mathcal{A}_{d_{\alpha\uparrow}^\dagger d_{\alpha\uparrow}}$  reflect these two resonant zero-energy modes, as well as the satellite peaks. Notice that the corresponding anomalous  $\mathcal{A}_{d_{\alpha\uparrow}^\dagger d_{\alpha\uparrow}^\dagger}$  and  $\mathcal{A}_{d_{\alpha\uparrow}d_{\alpha\uparrow}}$  are phase shifted by  $\pi$  by swapping sides.

$\mu_{R\uparrow} = 0$  (purple line cuts) solely  $\gamma_{L2}$  and  $\gamma_{R1}$  couple to each other and build a MF dimer. This consists of a type of molecule without the mode  $\omega = 0$  and with the split levels bounding and anti-bounding states represented by bottom and top arcs in both the panels (b) and (d) of Fig.2. In Fig.2, see the cyan line cuts as the example of the MF dimer. The opposite situation is found in  $\mathcal{A}_{\gamma_{R2}}$  of Fig. 2(e), which identifies the isolated MBS  $\gamma_{R2}$  (purple line cut). Upon varying  $\mu_{R\uparrow}$ , the MF trimer composed by  $\gamma_{L2}$ ,  $\gamma_{R1}$  and  $\gamma_{R2}$  is established instead. The trimer formation is symbolized by panels (b), (d) and (e) of Fig.2, where the bonding (bottom arc) and anti-bonding (top arc) states appear together with the mode at  $\omega = 0$ , the so-called non-bonding, also in Figs.2(b) and (e). To note this, see in Fig.2 the green line cuts as the example of the MF trimer. In this manner, the “Poor M.M. regime” emerges, being characterized by the amplitude of  $\mathcal{A}_{\gamma_{R2}}$  at  $\omega = 0$  that decreases while the corresponding in  $\mathcal{A}_{\gamma_{L2}}$  increases by changing  $\mu_{R\uparrow}$ . It means that the initially isolated MBS  $\gamma_{R2}$  at the right QD spills over the left QD and becomes the “Poor M.M.” [47]. Such a behavior is also recorded in  $\mathcal{A}_{d_{L\uparrow}d_{L\uparrow}^\dagger}$  and  $\mathcal{A}_{d_{R\uparrow}d_{R\uparrow}^\dagger}$ , which at the *sweet spot* with  $\mu_{R\uparrow} = 0$  compete at equal footing, i.e.,  $\mathcal{A}_{d_{L\uparrow}d_{L\uparrow}^\dagger}(0) = \mathcal{A}_{d_{R\uparrow}d_{R\uparrow}^\dagger}(0)$ . However, the “Poor M.M. regime”  $\mu_{R\uparrow} \neq 0$ , the imbalance  $\mathcal{A}_{d_{R\uparrow}d_{R\uparrow}^\dagger}(0) < \mathcal{A}_{d_{L\uparrow}d_{L\uparrow}^\dagger}(0)$  takes place due to the spill over-like behavior from  $\gamma_{R2}$  to  $\gamma_{L2}$ .

Fig.3 makes explicit the *sweet spot*. Particularly, Figs.3(a) and (c) show the features of  $\gamma_{L1}$  and  $\gamma_{R2}$  that

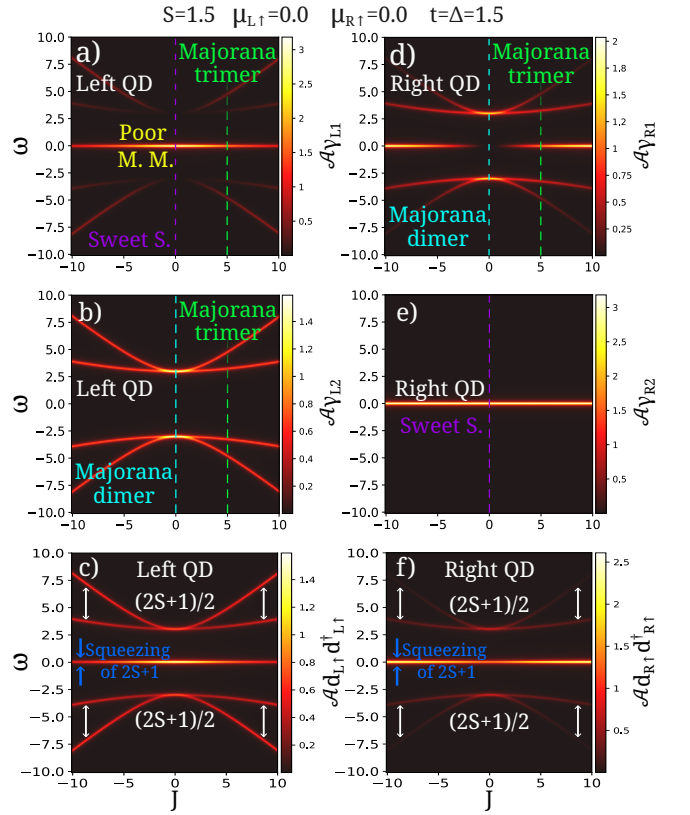


Figure 4. Color maps of  $\mathcal{A}_{d_{\alpha\uparrow}d_{\alpha\uparrow}^\dagger}$  and  $\mathcal{A}_{\gamma_{\alpha j}}$  in the “Majorana chain regime” spanned by  $\omega_{\alpha\uparrow}$  and  $J$  showing our main finding: in the presence of the quantum spin  $S$ , half of the fine structure is made explicit. The spill over-like behavior of the zero-energy mode of the “Poor Man’s Majorana” continues and the mode is protected against  $J$ . Such a phenomenon is due to the other half that squeezes itself as the “Poor Man’s Majorana” at  $\omega = 0$  and avoids the mixing with the latter.

clearly reveal the resonant states at  $\omega = 0$ , thus corresponding to the purple line cuts marked in Fig.2(a) and (e), respectively. On the other hand,  $\gamma_{L2}$  also presented in Fig.3(a), exhibits two resonant states around  $\omega = 0$  instead, due to the finite coupling  $t = \Delta$  of the MF dimer made by  $\gamma_{L2}$  and  $\gamma_{R1}$ . As aftermath, the same behavior of  $\gamma_{L2}$  is followed by  $\gamma_{R1}$ , as can be verified in Fig.3(c). It means that two isolated MBSs  $\gamma_{L1}$  and  $\gamma_{R2}$  are spatially apart at the left and right QDs, respectively. For completeness, in Figs.3(b) and (d) we summarize the spectral profiles of the GFs  $\mathcal{A}_{d_{\alpha\uparrow}d_{\alpha\uparrow}^\dagger}$ ,  $\mathcal{A}_{d_{\alpha\uparrow}^\dagger d_{\alpha\uparrow}}$ ,  $\mathcal{A}_{d_{\alpha\uparrow}^\dagger d_{\alpha\uparrow}^\dagger}$  and  $\mathcal{A}_{d_{\alpha\uparrow}d_{\alpha\uparrow}}$  of the QDs. Interestingly enough, the anomalous GFs, namely  $\mathcal{A}_{d_{\alpha\uparrow}^\dagger d_{\alpha\uparrow}^\dagger}$  and  $\mathcal{A}_{d_{\alpha\uparrow}d_{\alpha\uparrow}}$ , exhibit spectral profiles shifted by  $\pi$  by making the swap  $L \leftrightarrow R$ , once these GFs depend on the parity of the QD site.

Now in Fig.4 we discuss our main finding by introducing the *protection-like* behavior observed in the zero-energy mode arising from the “Poor M.M.”. For such an analysis, we consider  $S = 1.5$ ,  $\mu_{L\uparrow} = \mu_{R\uparrow} = 0$  and evaluate the spectral densities spanned by  $\omega$  and  $J$ . We call

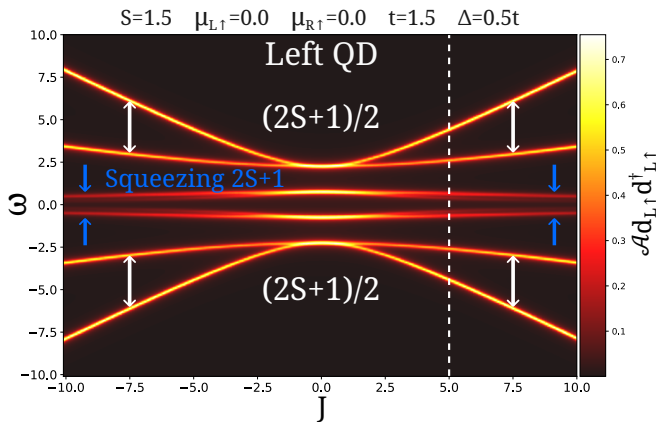


Figure 5. Color map of  $\mathcal{A}_{d_{L\uparrow}d_{L\uparrow}^\dagger}$  off the “Majorana chain regime” spanned by  $\omega$  and  $J$  showing the squeezing mechanism of half of the fine structure towards  $\omega = 0$  to form the “Poor Man’s Majorana”. As expected, the fine structure contains the amount of  $2 \times (2S + 1)$  levels, but for  $|J| \sim 5$ . The inner  $(2S + 1)$  makes explicit a trend to merge as a zero mode.

attention that, according to Eq.(2), the exchange  $J$  plays the role of an effective chemical potential acting over the left QD. It means that when  $J = 0$  the *sweet spot* is restored and we have again the MF dimer  $\gamma_{L2}$  and  $\gamma_{R1}$ , with the non-local and isolated  $\gamma_{L1}$  and  $\gamma_{R2}$  at the left and right QDs, respectively. However for  $J \neq 0$ , the MF trimer becomes now composed by  $\gamma_{L1}, \gamma_{L2}$  and  $\gamma_{R1}$ , thus driving the system into the “Poor M.M. regime”, where the novel “Poor M.M.” is expected to be  $\gamma_{L1}$ .

We begin the numerical analysis with  $\mathcal{A}_{\gamma_{L1}}$  and  $\mathcal{A}_{\gamma_{R2}}$  in Figs.4(a) and (e), which due to the  $J = 0$  condition, gives rise to the non-local and isolated MBSs  $\gamma_{L1}$  and  $\gamma_{R2}$  (purple line cuts), respectively. These MBSs are represented by the finite and equally amplitudes for the zero-energy mode at  $\omega = 0$ . With  $J = 0$ ,  $\mathcal{A}_{\gamma_{L2}}$  and  $\mathcal{A}_{\gamma_{R1}}$  display a split-peak structure as a function of  $\omega$ , once  $\gamma_{L2}$  and  $\gamma_{R1}$  builds the MF dimer (cyan line cuts in Figs.4(b) and (d)). For  $J \neq 0$  and  $\omega \neq 0$ , extra bottom and top arcs rise in Figs.4(a), (b) and (d) for  $\mathcal{A}_{\gamma_{L1}}, \mathcal{A}_{\gamma_{L2}}$ , and  $\mathcal{A}_{\gamma_{R1}}$ , respectively, as a consequence of the MF trimer formation (green line cuts). Particularly, the amount of arcs is  $2S + 1$  due to the quantum spin and it corresponds to half of the fine structure expected. This issue we shall address later on. The spill over-like behavior of  $\gamma_{L1}$  on  $\gamma_{R1}$  can be noted in Figs.4(a) and (d), where the unbalance  $\mathcal{A}_{\gamma_{L1}}(0) < \mathcal{A}_{\gamma_{R1}}(0)$  is notorious away from  $J = 0$ . In this manner, we reveal that the zero mode of the “Poor M.M.” continues to spill over from one QD to another, being induced by  $J$ , but with the mode pinned at  $\omega = 0$  despite the strength of  $J$ . Thus, the zero-energy mode of the “Poor M.M.” does not mix with the explicit  $2S + 1$  fine structure and characterizes the feature under protection against  $J$  coupling.

Back to the fine structure subject, we highlight that the bonding (bottom arc) and anti-bonding (top arc) states of Figs.2(c) and (f) are expected to split into  $2S + 1$

levels each in the presence of the quantum spin  $S$ . However, such a value is renormalized by its half  $(2S + 1)/2$ , as marked by the double arrows in Figs.4(c) and (f). It means that the other half is kept squeezed at  $\omega = 0$  as the zero-energy mode of the “Poor M.M.” and consequently, it ensures its pinning there, as well as the protection against the remaining fine structure. From experimental perspective, the unbalance  $\mathcal{A}_{d_{\alpha\uparrow}d_{\alpha\uparrow}^\dagger}(0) < \mathcal{A}_{d_{\bar{\alpha}\uparrow}d_{\bar{\alpha}\uparrow}^\dagger}(0)$  off  $J = 0$  and absence of mixing characteristic with the explicit half of the fine structure would emerge as the hallmarks of the “Poor M.M.” at the QD  $\alpha$  exchange coupled to the quantum spin.

In order to elucidate the aforementioned squeezing mechanism of half of the fine structure responsible to build the “Poor M.M.”, in Fig.5 we present  $\mathcal{A}_{d_{L\uparrow}d_{L\uparrow}^\dagger}$  for the case  $\Delta = 0.5t$ , which corresponds to a situation off the “Majorana chain regime”. It is worth mentioning that the exhibition of  $\mathcal{A}_{d_{R\uparrow}d_{R\uparrow}^\dagger}$  is redundant, once it shares the same features observed in  $\mathcal{A}_{d_{L\uparrow}d_{L\uparrow}^\dagger}$ . Additionally, we would like to remind that due to the quantum spin  $S$ , the dimer of QDs of Fig.1 is predicted to exhibit  $2 \times (2S + 1)$  levels for  $J \neq 0$ , where the number 2 accounts for the bounding and anti-bounding states. Therefore, as we can observe in Fig.5, this quantity of levels appears as expected, but resolved just around  $|J| \sim 5$ . This set is surprising, once it reveals the trend of the inner fine structure, which delimits precisely the half  $2S + 1$  levels from the entire fine structure nearby  $\omega = 0$ . We call attention that the pattern of this inner portion precedes the formation of the “Poor M.M.”, which is complete in the “Majorana chain regime”  $\Delta = t$  of Fig.4 with all these  $2S + 1$  inner levels squeezed at  $\omega = 0$ . In this manner, we point out that the inner half-structure is squeezing towards  $\omega = 0$  to end-up as the zero-energy mode of the “Poor M.M.” upon approaching  $\Delta \rightarrow t$ . Particularly for  $\Delta \neq t$ , the anti-crossing point at  $J = 0$  of the inner levels arises from the existence of two MF dimers, namely  $\gamma_{L2}, \gamma_{R1}$  and  $\gamma_{L1}, \gamma_{R2}$ .

For completeness, we clarify that the case of the half-integer  $S$  here adopted does not cause loss of generality. In the situation of an integer spin, the explicit fine structure would have only the mode  $\omega = 0$  degenerate with the corresponding squeezed at this point instead and the phenomenon reported would be still observable.

To summarize, in the Supplemental Material we have prepared an animated plot for the vertical line cut depicted in Fig.5, where the crossover from the regime  $\Delta = 0$ , with the  $2 \times (2S + 1)$  fine structure, evolves towards the situation  $\Delta = t$ , in which the half  $(2S + 1)$ , then leads to the “Poor M.M.” at  $\omega = 0$ .

*Conclusions.-* We reveal in the system of two superconducting QDs that the “Poor Man’s Majorana” exhibits a local protection against the spin splitting when its host QD is exchange coupled to a quantum spin. Two key features ensure such a protection. First, the MBS zero mode consistently remains at zero frequency regardless of the coupling strength with the spin. Second, the

unexpected half of the fine structure does not eliminate the zero-energy mode. We attribute such a behavior to the squeezing phenomenon of the other half as the zero-energy mode of the “*Poor Man’s Majorana*”. It keeps the mode detached from the remaining and observable portion of the fine structure, making the MBS protected. Our findings pave the way in highlighting that such a MBS is robust against the generally supposed unavoidable split by the fine structure from the spin. To conclude, we understand that these results shift the lack of topological protection paradigm of the “*Poor Man’s Majorana*”, thereby unveiling new possibilities for this quasiparticle.

*Acknowledgments.*- We thank the Brazilian fund-

ing agencies CNPq (Grants. Nr. 302887/2020-2, 303772/2023-9, 311980/2021-0, and 308695/2021-6), the São Paulo Research Foundation (FAPESP; Grant No. 2023/13467-6), Coordenação de Aperfeiçoamento de Pessoal de Nível Superior - Brasil (CAPES) – Finance Code 001 and FAPERJ process Nr. 210 355/2018. LSR acknowledges the support from the Icelandic Research Fund (Rannís), Grant No. 239552-051. LSR thanks Unesp for their hospitality. HS acknowledges the project No. 2022/45/P/ST3/00467 co-funded by the Polish National Science Centre and the European Union Framework Programme for Research and Innovation Horizon 2020 under the Marie Skłodowska-Curie grant agreement No. 945339.

- 
- [1] E. Majorana, *Il Nuovo Cimento* (1924-1942) **14**, 10.1007/BF02961314 (1937).
- [2] P. Marra, *Journal of Applied Physics* **132**, 231101 (2022).
- [3] E. Vernek, P. H. Penteado, A. C. Seridonio, and J. C. Egues, *Phys. Rev. B* **89**, 165314 (2014).
- [4] O. Lesser and Y. Oreg, *Journal of Physics D: Applied Physics* **55**, 164001 (2022).
- [5] F. Pientka, L. I. Glazman, and F. von Oppen, *Phys. Rev. B* **89**, 180505 (2014).
- [6] Y. Oreg, G. Refael, and F. von Oppen, *Phys. Rev. Lett.* **105**, 177002 (2010).
- [7] F. Pientka, L. I. Glazman, and F. von Oppen, *Phys. Rev. B* **88**, 155420 (2013).
- [8] J. Klinovaja, P. Stano, A. Yazdani, and D. Loss, *Phys. Rev. Lett.* **111**, 186805 (2013).
- [9] S. Nadj-Perge, I. K. Drozdov, B. A. Bernevig, and A. Yazdani, *Phys. Rev. B* **88**, 020407 (2013).
- [10] L. Fu and C. L. Kane, *Phys. Rev. B* **79**, 161408 (2009).
- [11] L. Fu and C. L. Kane, *Phys. Rev. Lett.* **100**, 096407 (2008).
- [12] M. M. Vazifeh and M. Franz, *Phys. Rev. Lett.* **111**, 206802 (2013).
- [13] S. Nakosai, Y. Tanaka, and N. Nagaosa, *Phys. Rev. B* **88**, 180503 (2013).
- [14] B. Braunecker and P. Simon, *Phys. Rev. Lett.* **111**, 147202 (2013).
- [15] A. C. Potter and P. A. Lee, *Phys. Rev. B* **85**, 094516 (2012).
- [16] S. B. Chung, H.-J. Zhang, X.-L. Qi, and S.-C. Zhang, *Phys. Rev. B* **84**, 060510 (2011).
- [17] C. W. J. Beenakker, *Rev. Mod. Phys.* **87**, 1037 (2015).
- [18] M. Sato and S. Fujimoto, *Journal of the Physical Society of Japan* **85**, 072001 (2016).
- [19] M. Sato and Y. Ando, *Reports on Progress in Physics* **80**, 076501 (2017).
- [20] A. Haim and Y. Oreg, *Physics Reports* **825**, 1 (2019), time-reversal-invariant topological superconductivity in one and two dimensions.
- [21] J. Alicea, *Reports on Progress in Physics* **75**, 076501 (2012).
- [22] C. Beenakker, *Annual Review of Condensed Matter Physics* **4**, 113 (2013).
- [23] A. S. Karsten Flensberg, Felix von Oppen, *Nature Reviews Materials* **6**, 944 (2021).
- [24] K. Laubscher and J. Klinovaja, *Journal of Applied Physics* **130**, 081101 (2021).
- [25] M. T. Deng, S. Vaitiekėnas, E. B. Hansen, J. Danon, M. Leijnse, K. Flensberg, J. Nygard, P. Krogstrup, and C. M. Marcus, *Science* **354**, 1557 (2016).
- [26] V. Mourik, K. Zuo, S. M. Frolov, S. R. Plissard, E. P. A. M. Bakkers, and L. P. Kouwenhoven, *Science* **336**, 1003 (2012).
- [27] F. Nichele, A. C. C. Drachmann, A. M. Whiticar, E. C. T. O’Farrell, H. J. Suominen, A. Fornieri, T. Wang, G. C. Gardner, C. Thomas, A. T. Hatke, P. Krogstrup, M. J. Manfra, K. Flensberg, and C. M. Marcus, *Phys. Rev. Lett.* **119**, 136803 (2017).
- [28] A. Y. Kitaev, *Physics-Uspekhi* **44**, 131 (2001).
- [29] R. Aguado, *LA RIVISTA DEL NUOVO CIMENTO* **40**, 523 (2017).
- [30] S. R. Elliott and M. Franz, *Rev. Mod. Phys.* **87**, 137 (2015).
- [31] M. Leijnse and K. Flensberg, *Semiconductor Science and Technology* **27**, 124003 (2012).
- [32] T. D. Stanescu and S. Tewari, *Journal of Physics: Condensed Matter* **25**, 233201 (2013).
- [33] B. Jack, Y. Xie, and A. Yazdani, *Nature Reviews Physics* **3**, 2522 (2021).
- [34] R. Pawlak, M. Kisiel, J. Klinovaja, T. Meier, S. Kawai, T. Glatzel, D. Loss, and E. Meyer, *npj Quantum Information* **2**, 10.1038/npjqi.2016.35 (2016).
- [35] M. Ruby, F. Pientka, Y. Peng, F. von Oppen, B. W. Heinrich, and K. J. Franke, *Phys. Rev. Lett.* **115**, 197204 (2015).
- [36] T.-P. Choy, J. M. Edge, A. R. Akhmerov, and C. W. J. Beenakker, *Phys. Rev. B* **84**, 195442 (2011).
- [37] J. Klinovaja, P. Stano, A. Yazdani, and D. Loss, *Phys. Rev. Lett.* **111**, 186805 (2013).
- [38] S. Nadj-Perge, I. K. Drozdov, J. Li, H. Chen, S. Jeon, J. Seo, A. H. MacDonald, B. A. Bernevig, and A. Yazdani, *Science* **346**, 602 (2014).
- [39] S. Jeon, Y. Xie, J. Li, Z. Wang, B. A. Bernevig, and A. Yazdani, *Science* **358**, 772 (2017).
- [40] P. Marra and M. Nitta, *Phys. Rev. B* **100**, 220502 (2019).
- [41] R. Pawlak, S. Hoffman, J. Klinovaja, D. Loss, and E. Meyer, *Progress in Particle and Nuclear Physics* **107**, 1 (2019).
- [42] G. Górski, J. Baranski, I. Weymann, and T. Domanski,

- Scientific Reports **8**, 15717 (2018).
- [43] R. M. Lutchyn, J. D. Sau, and S. Das Sarma, *Phys. Rev. Lett.* **105**, 077001 (2010).
- [44] T. Dvir, G. Wang, N. van Loo, C.-X. Liu, G. P. Mazur, A. Bordin, S. L. D. ten Haaf, S. L. D. ten Haaf, J.-Y. Wang, D. van Driel, F. Zatelli, X. Li, F. K. Malinowski, S. Gazibegovic, G. Badawy, E. P. A. M. Bakkers, M. Wimmer, and L. P. Kouwenhoven, *Nature* **614**, 445 (2023).
- [45] S. L. D. ten Haaf, Q. Wang, A. M. Bozkurt, C.-X. Liu, I. Kulesh, P. Kim, D. Xiao, C. Thomas, M. J. Manfra, T. Dvir, M. Wimmer, and S. Goswami, *Nature* **630**, 329 (2024).
- [46] A. Bordin, C.-X. Liu, T. Dvir, F. Zatelli, S. L. D. ten Haaf, D. van Driel, G. Wang, N. van Loo, T. van Caekenberghe, J. C. Wolff, Y. Zhang, G. Badawy, S. Gazibegovic, E. P. A. M. Bakkers, M. Wimmer, L. P. Kouwenhoven, and G. P. Mazur, *Signatures of majorana protection in a three-site kitaev chain* (2024), [arXiv:2402.19382](https://arxiv.org/abs/2402.19382) [cond-mat.supr-con].
- [47] M. Leijnse and K. Flensberg, *Phys. Rev. B* **86**, 134528 (2012).
- [48] A. Tsintzis, R. S. Souto, and M. Leijnse, *Phys. Rev. B* **106**, L201404 (2022).
- [49] A. Tsintzis, R. S. Souto, K. Flensberg, J. Danon, and M. Leijnse, *PRX Quantum* **5**, 010323 (2024).
- [50] R. S. Souto, A. Tsintzis, M. Leijnse, and J. Danon, *Phys. Rev. Res.* **5**, 043182 (2023).
- [51] M. Luethi, H. F. Legg, D. Loss, and J. Klinovaja, *From perfect to imperfect poor man's majoranas in minimal kitaev chains* (2024), [arXiv:2408.03071](https://arxiv.org/abs/2408.03071) [cond-mat.mes-hall].
- [52] M. Luethi, H. F. Legg, D. Loss, and J. Klinovaja, *The fate of poor man's majoranas in the long kitaev chain limit* (2024), [arXiv:2408.10030](https://arxiv.org/abs/2408.10030) [cond-mat.mes-hall].
- [53] S. G. BRUSH, *Rev. Mod. Phys.* **39**, 883 (1967).
- [54] H. Bruus and K. Flensberg, (Oxford: Oxford University Press) (2012).